



7th International Conference on Silicon Photovoltaics, SiliconPV 2017

Introducing pinhole magnification by selective etching: application to poly-Si on ultra-thin silicon oxide films

Dominic Tetzlaff^{a,*}, Marvin Dzinnik^a, Jan Krügener^a, Yevgeniya Larionova^b, Sina Reiter^b, Mircea Turcu^b, Robby Peibst^{a,b}, Uwe Höhne^c, Jan-Dirk Kähler^c, Tobias F. Wietler^{a,d}

^a*Institute of Electronic Materials and Devices, Leibniz Universität Hannover, D-30167 Hannover*

^b*Institute for Solar Energy Research Hamelin, D-31860 Emmerthal*

^c*centrotherm photovoltaics AG, D-30179 Hannover*

^d*Laboratory of Nano and Quantum Engineering, Leibniz Universität Hannover, D-30167 Hannover*

Abstract

Carrier selective junctions formed by polycrystalline silicon (poly-Si) on ultra-thin silicon oxide films are currently in the spotlight of silicon photovoltaics. We develop a simple method using selective etching and conventional optical microscopy to determine the pinhole density in interfacial oxide films of poly-Si on oxide (POLO)-junctions with excellent electrical properties. We characterize the selective etching of poly-Si versus ultra-thin silicon oxide. We use test structures with deliberately patterned openings and 3 nm thin oxide films to check the feasibility of magnification by undercutting the interfacial oxide. With the successful proof of our concept we introduce a new method to access the density of nanometer-size pinholes in POLO-junctions with excellent passivation properties.

© 2017 The Authors. Published by Elsevier Ltd.

Peer review by the scientific conference committee of SiliconPV 2017 under responsibility of PSE AG.

Keywords: polysilicon; carrier selective contacts; pinholes; Tetramethylammonium hydroxide (TMAH)

* Corresponding author. Tel.: +49-511-7625037; fax: +49-511-7624229.

E-mail address: tetzlaff@mbe.uni-hannover.de

1. Introduction

Carrier selective junctions formed by polycrystalline silicon-rich layers on ultra-thin silicon oxide films are currently in the spotlight of silicon photovoltaics research. Remarkable junction passivation and low specific contact resistances [1,2] have enabled conversion efficiencies of 25.3% with the TOPCon-approach for one carrier polarity [3] and 25.0% applying poly-Si on oxide (POLO)-junctions for both carrier polarities [4].

A plethora of models has been developed to explain the basic principle behind the carrier selectivity of POLO-junctions since their first application to silicon bipolar junction transistors decades ago [5,6]. The break-up of the interfacial oxide film under annealing has been identified as a crucial process step to achieve high quality junctions [7,8]. On the one hand the formation of holes in the oxide film has been regarded as detrimental to the electrical junction properties [9]. On the other hand localized carrier transport through pinholes in the interfacial oxide has been discussed as a key mechanism beside direct tunneling [10,11]. So, the determination of size and density of pinholes in POLO-junctions with good electrical properties would be an important step towards a more accurate description of the current transport mechanism and predictive modelling of the junction formation process. Practically, optimization strategies might be deduced from the knowledge of the microstructural properties and their dependency on process parameters.

Unfortunately, finding nanometer-size pinholes at densities below 10^9 cm^{-2} , as expected for a POLO-junction with good electrical properties [10], is very challenging. In a recent transmission electron microscopy (TEM) study it was possible to identify about 5 nm small regions of direct contact between the crystalline silicon and the poly-Si layer in POLO-junctions with excellent passivation properties [12]. TEM only allows an approximate estimation of the density of these regions [12]. Clearly, a less uncertain method to measure the pinhole density is required. One approach could be conductive atomic force microscopy [13]. One limitation of this method is the lateral conductivity of the poly-Si films, which has to be small in order to enable the required resolution. Another approach, which circumvents the latter constraint, is presented here. We combine selective etching and simple optical microscopy (OM). First, the poly-Si has to be removed without harming the ultra-thin silicon oxide film underneath to make the pinholes accessible by OM. This requires a highly selective etching process. We use tetramethylammonium hydroxide (TMAH) which is frequently used in microelectronics and micromechanics as an anisotropic etchant for silicon and known for high selectivity to silicon oxide. Secondly, nanometer-size pinholes have to be magnified to the micrometer range for OM detection. We exploit the fact that openings in the oxide film result in undercutting for overetching conditions. This can yield etch pits large enough to be visible in OM. The feasibility of this second step is demonstrated in a proof of principle experiment using lithographically patterned openings in a less than 3 nm thin silicon oxide film.

2. Experimental

Two sets of samples were prepared for optimizing the selectivity between silicon and silicon oxide for etching with TMAH solution. On a first set of silicon wafers, a dry thermal oxide with a thickness above 50 nm was grown at 1000 °C. These wafers were used to determine the etch rates of TMAH for SiO_2 . A second set of wafers was prepared to measure the TMAH etch rate for poly-Si films. Therefore, etch stop layers were applied (SiN_x or SiO_2), whose only purpose is to prevent etching into the silicon wafer after complete removal of the poly-Si layers. The latter were prepared by low pressure chemical vapor deposition (LPCVD) with thicknesses of 100 - 220 nm. Besides intrinsic poly-Si, phosphorous and boron doped poly-Si layers were produced *in situ* (n , p^+) or using ion implantation (p). The dopant concentrations are above $6 \cdot 10^{19} \text{ atoms/cm}^3$ for the *in situ* doped n poly-Si layers, $3 \cdot 10^{19} \text{ atoms/cm}^3$ for the ion implanted p poly-Si layers and above the solid solubility limit for the *in situ* boron doped p^+ polysilicon layers.

The etch rates of TMAH for poly-Si and SiO_2 were determined for different temperatures (70 °C, 80 °C and 90 °C) and concentrations (5%, 10%, 15% and 25%). All wafers were separated into several pieces and the thicknesses of silicon oxide and poly-Si were determined by spectroscopic ellipsometry. After etching in TMAH, the thicknesses were measured again, to determine the etching rate within certain time intervals.

To prove that the selectivity is sufficiently high for undercutting and thus magnifying openings in the oxide, a 10 nm thick thermal oxide on Si wafers was lithographically patterned to produce holes with edge lengths of 1 μm

and 4 μm . After photoresist removal, an HF cleaning step reduced the oxide thickness to about 3 nm prior to the LPCVD of 150 nm poly-Si followed by ion implantation of elemental boron (10 keV, $5 \cdot 10^{14}$ atoms/cm²). After etching in TMAH with optimized parameters, these samples were characterized with OM and scanning electron microscopy (SEM).

3. Results and discussion

Several groups have studied the etch rates of single-crystalline Si using TMAH [14-17]. The highest etch rates for Si(100) surfaces are expected for 5-8% TMAH etching solution at 90 °C while they decrease with increasing TMAH concentration [14,16,17]. The etch rate is expected to be higher for polycrystalline than for single-crystalline Si [18]. However, doping concentration has also a huge impact, drastically reducing the Si etch rate for boron concentrations above 10^{19} atoms/cm³ [18]. To ensure that the TMAH etching procedure is suitable for pinhole detection in POLO-junctions, a very high selectivity between poly-Si and SiO₂ is needed. Therefore we start our investigations with *in situ* boron doped poly-Si films with doping concentrations above the solid solubility limit, which should lead to the lowest poly-Si etching rates. Fig. 1(a) shows the corresponding etch rates for TMAH concentrations of 5%, 10% and 15%. The TMAH concentration of 25% is not shown, as there is no noteworthy removal of poly-Si. The etch rate increases with temperature in accordance to literature [14]. However, we observe an increasing etch rate with increasing TMAH concentration, leading to the highest etch rate of 1.9 nm/s for 15% TMAH at 90 °C. Another effect exists when etching samples with extremely high boron concentrations. For some samples the poly-Si thickness is not reduced within the first minutes while others show no poly-Si removal at all. This indicates the presence of a TMAH resistant layer at the surface. During the annealing step at 950 °C in nitrogen ambient a boron rich layer could have formed, as reported in literature for different furnace processes [19-21]. However, after removing the top 10 nm of the layer using an argon sputtering process, etching with TMAH becomes possible immediately.

For comparison, the etch rate for the ion-implanted samples (boron concentration of $3 \cdot 10^{19}$ atoms/cm³ assuming homogeneous distribution of the implanted ion dose) is also shown in Fig. 1(a). However, as the etch rate is much higher, the whole poly-Si layer is removed completely within seconds. Therefore the etch rate of 10 nm/s is only a lower limit, while much higher etch rates are expected (as indicated by the arrow).

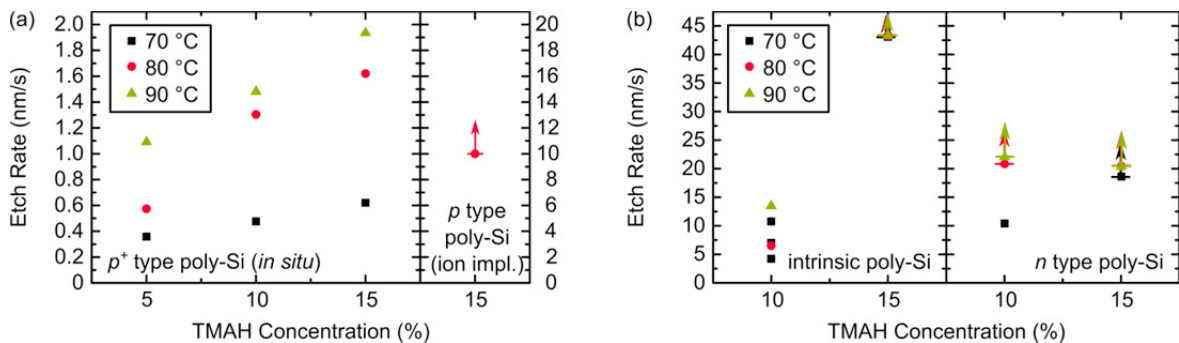


Fig. 1. (a) TMAH etch rates for *p*⁺ / *p* type boron doped layers; (b) TMAH etch rates for intrinsic and *n* type phosphorous doped layers.

Fig. 1(b) shows the corresponding TMAH etch rates for intrinsic and *n* type poly-Si. As seen for the *in situ* boron doped samples, the etch rates using 15% TMAH concentration are higher than for 10%. The highest rates achieved are 43 nm/s for intrinsic and 22 nm/s for *n* poly-Si. The arrows again indicate that for some samples the true etch rates will be even higher, as the poly-Si layer is removed completely within seconds. These lower limits of the etch rates correspond well to the highest TMAH etch rates of single-crystalline Si reported by several groups [14,16,17] but for different concentrations of 5-8% at 90 °C. This difference in concentration for highest etch rates could be an effect introduced by the polycrystalline structure of our samples.

Our findings for the etch rate of SiO₂ are shown in Fig. 2(a). The etch rate also increases with increasing temperature. In contrast to the poly-Si layers discussed before, the etch rate drops with increasing TMAH concentration and reaches a minimum at 15%. Why the etch rates slightly increases for TMAH concentration of 25% is not clear right now. However, the etch rates determined for concentrations up to 15% correlate well with the results of Tabata *et al.* [14].

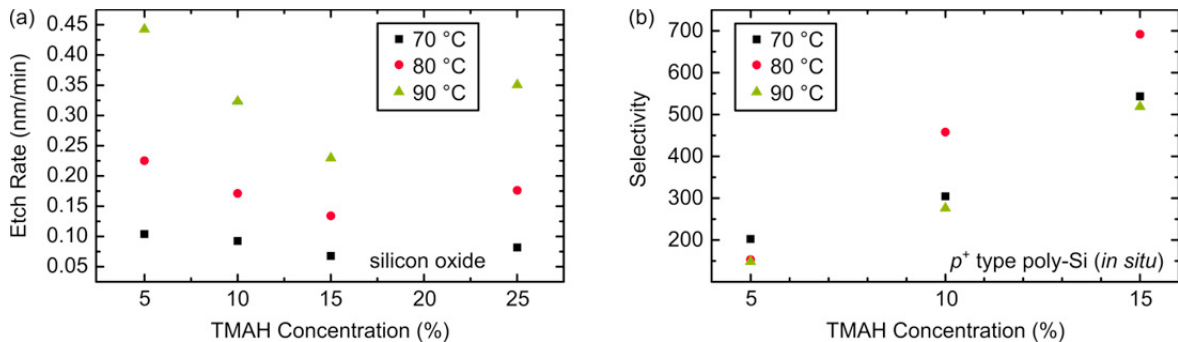


Fig. 2. (a) TMAH etch rates for SiO₂; (b) Selectivity for *in situ* p⁺ type doped layers.

As our goal is to investigate samples with poly-Si layers of up to 150 nm on top of thin oxides of about 1.5 nm a selectivity of about 1000:1 for TMAH etching of poly-Si versus SiO₂ would be sufficient for undercutting the oxide such that every pinhole should lead to an etch pit with strongly enlarged dimensions. As the *in situ* boron doped samples have the lowest etch rates, the values shown in Fig. 2(b) are the lower limits of the selectivity. The latter increases with increasing temperature as well as with concentration. The selectivity for a TMAH concentration of 25% is not shown, as there was no noteworthy removal of poly-Si. The selectivity increases if the dopant concentration of boron is reduced. For phosphorous doped and intrinsic poly-Si it is much higher (> 10000:1). However, even for boron concentrations above the solid solubility limit the selectivity seems to be sufficiently high for undercutting an ultra-thin oxide without massively reducing the oxide thickness.

To test the stability of ultra-thin oxide films and to prove the concept of pinhole magnification by undercutting lithographically patterned samples are prepared as described above. Fig. 3(a) shows an excerpt of the mask used to produce openings with 1 μm and 4 μm edge length and two types of larger alignment marks (negative mark: only the cross will be etched; positive mark: everything besides the cross will be etched). Successful patterning of the silicon oxide film was confirmed by OM (not shown here) prior to poly-Si LPCVD and ion implantation. Fig. 3(b) shows an OM image of the patterned area after removal of the native oxide with HF solution and subsequent etching with 15% TMAH solution at 80 °C. The poly-Si has been completely removed and all structures of the mask are found. No additional contrasts are observed indicating immunity of the 3 nm thin silicon oxide film versus the etching process. The shape of the alignment marks differs from the original mask pattern. This is due to the etch rate anisotropy for different crystallographic directions in TMAH etching of the monocrystalline silicon beneath the silicon oxide film. While the cross shape of the upper negative marks is still visible, it is completely removed in the lower positive mark. This is confirmed in the cross-sectional SEM image of a positive alignment mark shown in Fig. 3(c). The etch pit's sidewalls correspond to (111) planes. Measuring the vertical and lateral dimensions yields a selectivity of 10 – 30 between the [001] and [111] directions. The edge length of the etch pit is more than one micrometer larger than the original patterned size measured in the silicon oxide film before the TMAH etching step (not shown here). This proves the concept of magnification of oxide openings by undercutting. An etch pit enlargement of more than a micrometer as achieved here, will be sufficient for easy OM detection when applied to nanometer-size pinholes.

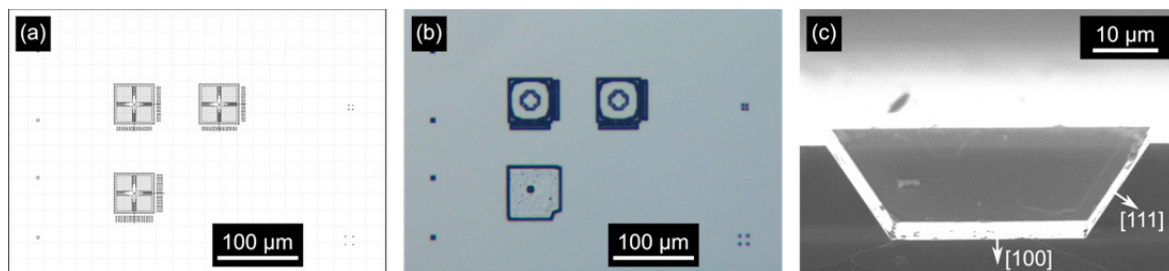


Fig. 3. (a) Excerpt of mask; (b) OM image of surface after etching with TMAH; (c) SEM image of etch pit of positive alignment mask.

4. Conclusions

Thanks to the high selectivity of TMAH, we can introduce overetching of poly-Si layers on ultra-thin silicon oxide films as a suitable method to magnify openings in the oxide for imaging by OM. Applying our process on poly-Si layers on ultra-thin silicon oxide films with openings deliberately produced by photolithography we found no additional contrasts in OM compared to the lithography mask used. This indicates that no additional holes were generated during the etching process. So, the determination of the pinhole density in POLO-junctions with excellent electrical properties becomes feasible. The method presented here can contribute another piece to the puzzle of the current transport mechanism in POLO junctions and eventually enable predictive modelling of the junction formation process. It was successfully applied to verify the existence of pinholes in the interfacial oxide in POLO junctions with excellent passivation quality [22].

Acknowledgements

This work was supported by the German Federal Ministry for Economic Affairs and Energy (BMWi) under contract no. 0325702B (POLO). We thank Guido Glowatzki, Andrea Lissel and Raymond Zieseniß for their help with sample processing.

References

- [1] Römer U, Peibst R, Ohrdes T, Lim B, Krügener J, Wietler T, Brendel R. Ion Implantation for Poly-Si Passivated Back-Junction Back-Contacted Solar Cells. *IEEE J. Photovolt.* 2015;5:507-514.
- [2] Larionova Y, Peibst R, Turcu M, Reiter S, Brendel R, Tetzlaff D, Krügener J, Wietler T, Höhne U, Kähler JD. Optimization of p+ poly-Si / c-Si junctions on wet-chemically grown interfacial oxides and on different wafer morphologies. *32nd EU PVSEC 2016*, Munich, Germany.
- [3] Richter A, Benick J, Feldmann F, Fell A, Hermle M, Glunz SW. Silicon solar cells with full-area passivated rear contact: Influence of base resistivity on device performance on a 25% efficiency level. *26th International PVSEC 2016*, Singapore.
- [4] Haase F, Kiefer F, Krügener J, Brendel R, Peibst R. IBC solar cells with polycrystalline on oxide (POLO) passivating contacts for both polarities. *26th International PVSEC 2016*, Singapore.
- [5] Post ICR, Ashburn P, Wolstenholme GR. Polysilicon emitters for bipolar transistors: a review and re-evaluation of theory and experiment. *IEEE Trans. Electron Dev.* 1992;39:1717-1731.
- [6] Rinaldi NF. On the modeling of polysilicon emitter bipolar transistors. *IEEE Trans. Electron Dev.* 1997;44:395-403 (1997).
- [7] Wolstenholme GR, Jorgensen N, Ashburn P, Booker GR. An investigation of the thermal stability of the interfacial oxide in poly-crystalline silicon emitter bipolar transistors by comparing device results with high-resolution electron microscopy observations. *J. Appl. Phys.* 1987;61:225-233.
- [8] Ajuria SA, Reif R. Early stage evolution kinetics of the polysilicon/single-crystal silicon interfacial oxide upon annealing. *J. Appl. Phys.* 1991;69:662-667.
- [9] Moldovan A, Feldmann F, Zimmer M, Rentsch J, Benick J, Hermle M. Tunnel oxide passivated carrier-selective contacts based on ultra-thin SiO₂ layers. *Sol. Energ. Mat. Sol. Cells* 2015;142:123-127.
- [10] Peibst R, Römer U, Hofmann KR, Lim B, Wietler TF, Krügener J, Harder NP, Brendel R. A Simple Model Describing the Symmetric I-V Characteristics of p Polycrystalline Si/n Monocrystalline Si, and n Polycrystalline Si/p Monocrystalline Si Junctions. *IEEE J. Photovolt.* 2014;4:841-850.

- [11] Peibst R, Römer U, Larionova Y, Rienäcker M, Merkle A, Folchert N, Reiter S, Turcu M, Min B, Krügener J, Tetzlaff D, Bugiel E, Wietler T, Brendel R. Working principle of carrier selective poly-Si/c-Si junctions: Is tunnelling the whole story? *Sol. Energ. Mat. Sol. Cells* 2016;158:60-67.
- [12] Tetzlaff D, Krügener J, Larionova Y, Reiter S, Turcu M, Peibst R, Höhne U, Kähler JD, Wietler T. Evolution of Oxide Disruptions: The (W)hole Story About Passivating Contacts. *43rd IEEE PVSC* 2016, Portland (OR), USA.
- [13] Lancaster K, Großer S, Feldmann F, Naumann V, Hagendorf C. Study of Pinhole Conductivity at Passivated Carrier-selected Contacts of Silicon Solar Cells. *Energy Procedia* 2016;92:116-121.
- [14] Tabata O, Asahi R, Funabashi H, Shimaoka K, Sugiyama S. Anisotropic etching of silicon in TMAH solutions. *Sens. Actuator A-Phys.* 1992;34:51-57.
- [15] Merlos A, Acero M, Bao MH, Bausells J, Esteve J. TMAH/IPA anisotropic etching characteristics. *Sens. Actuator A-Phys.* 1993;37:737-743.
- [16] Thong JTL, Choi WK, Chong CW. TMAH etching of silicon and the interaction of etching parameters. *Sens. Actuator A-Phys.* 1997;63:243-249.
- [17] Chen PH, Peng HY, Hsieh CM, Chyu MK. The characteristic behavior of TMAH water solution for anisotropic etching on both Silicon substrate and SiO₂ layer. *Sens. Actuator A-Phys.* 2001;93:132-137.
- [18] Charavel R, Laconte J, Raskin JP. Advantages of p⁺⁺ polysilicon etch stop layer versus p⁺⁺ silicon. *Proc. SPIE* 2003;5116:699-709.
- [19] Kessler MA, Ohrdes T, Wolpensinger B, Bock R, Harder NP. Characterisation and implications of the boron rich layer resulting from open-tube liquid source BBR3 boron diffusion processes. *34th IEEE PVSC* 2009, Philadelphia (PA), USA.
- [20] Singha B, Solanki CS. Impact of a boron rich layer on minority carrier lifetime degradation in boron spin-on dopant diffused n-type crystalline silicon solar cells. *Semicond. Sci. Technol.* 2016;31:035009
- [21] Kim C, Park S, Kim YD, Park H, Kim S, Kim H, Lee H, Kim D. Properties of boron-rich layer formed by boron diffusion in n-type silicon. *Thin Solid Films* 2014;564:253-257.
- [22] Tetzlaff D, Krügener J, Larionova Y, Reiter S, Turcu M, Haase F, Brendel R, Peibst R, Höhne U, Kähler JD, Wietler TF. A Simple Method for Pinhole Detection in Carrier Selective POLO-Junctions for High Efficiency Silicon Solar Cells. To be presented at 7th *SiliconPV* 2017, Freiburg, Germany.